Journal of Power Sources 196 (2011) 337–342

Contents lists available at ScienceDirect

Journal of Power Sources

journal homepage: www.elsevier.com/locate/jpowsour

Synthesis and electrochemical properties of $LiNi_{0.8}Co_{0.2}O_2$ nanopowders for lithium ion battery applications

Yaser Hamedi Jouybari, Sirous Asgari*

Department of Materials Science and Engineering, Sharif University of Technology, Azadi Ave., Tehran, P.O. Box 11155-9466, Iran

ARTICLE INFO

Article history:
Received 17 March 2010
Received in revised form 21 June 2010
Accepted 30 June 2010
Available online 7 July 2010

Keywords:
Sol–gel method
Nano-sized lithium–nickle–cobalt oxide
Cathode materials
Lithium ion batteries

ABSTRACT

Nitrates of lithium, cobalt and nickel are utilized to synthesize $LiNi_{0.8}Co_{0.2}O_2$ cathode material through sol–gel technique. Various synthesis parameters such as calcination time and temperature as well as chelating agent are studied to determine the optimized condition for material processing. Using TG/DTA techniques, the optimized calcination temperatures are selected. Different characterization techniques such as ICP, XRD and TEM are employed to characterize the chemical composition, crystal structure, size and morphology of the powders. Micron and nano-sized powders are produced using citric/oxalic and TEA as chelating agent, respectively. Selected powders are used as cathode material to assemble batteries. Charge–discharge testing of these batteries show that the highest discharge capacity is 173 mAh g^{-1} at a constant current of 0.1 mA cm^{-2}, between 3.0 and 4.2 V. This is obtained in a battery assembled with the nanopowder produced by TEA as chelating agent.

1. Introduction

Various types of cathode materials have been investigated for lithium battery applications. The intercalation compounds such as transition metal oxides, particularly $LiCoO_2$ [1–3], $LiNiO_2$ [4–6] and $LiMn_2O_4$ [5,7,8], have been developed because of their high output voltage (about 4 V) and good recharge capabilities. While $LiCoO_2$ is a common cathode material, problems such as toxic properties and high cost have driven researchers to look for other options. $LiMn_2O_4$ is considered as a candidate material to replace for $LiCoO_2$ but its low capacity and high reactivity with electrolyte at temperatures above 55 °C are major problems [9]. The third candidate for cathode materials is lithium nickel oxide. Difficulty in synthesis of layered stoichiometric $LiNiO_2$, however, is a major hurdle to its application in commercial lithium cells. This is due to the fact that Ni^{2+} (0.69 Å) and Li^+ (0.72 Å) ions are very close in size which favors partial substitution of nickel in Li layers. This arrangement hinders the easy movement of lithium ions [10,11] required for an effective charge–discharge process. Also, this material shows a phase transition during lithium deintercalation process (phase transition from an electrochemically active hexagonal phase to an inactive cubic phase) leading to irreversible capacity loss [5,12]. Research works have shown that substituting a part of nickel with a trivalent cation such as cobalt retards this undesired phase transition in nickel oxide [13–15]. A solid solution with a composition of $LiNi_xCo_{1-x}O_2$ ($0 < x < 1$) has a rhombohedral structure with $R\bar{3}m$ space group [12] and yields more stable cathode materials [16–21]. Due to its large capacity, good reversibility and low material cost [22–25], this compound has been widely studied as an alternative to the currently used cathode materials. Results have shown that for values of x around 0.2, the solid solution shows the best known electrochemical properties among the cathode materials discussed before [26]. The higher capacity of $LiNi_{0.8}Co_{0.2}O_2$ is mainly due to the fact that two thirds of lithium ions participate in the intercalation and deintercalation process. In $LiCoO_2$ only one-half of the lithium ions take part in these processes [27].

Electrochemical properties of cathode materials effectively depend on the synthesis route employed. While solid-state reaction has been widely used in the literature as a production route, problems such as inhomogeneity, irregular morphology, larger particle size, poor control of stoichiometry and a longer period of calcination have justified recent efforts to develop other processing techniques such as sol–gel process. This technique has several advantages such as low calcination temperature, shorter processing time and possibility of producing particles with sub-micron sizes with a narrow size distribution [28–32]. On the other hand, it has been proposed that electrodes made by nanopowders show a decrease in charge transfer resistance and an improvement in rate capabilities due to larger surface area. This leads to higher power output which is necessary for large electric equipments [33,34]. Also, the larger surface area of the nanopowders increases the discharge potential compared to that of micro powders [35].

In this study, $LiNi_{0.8}Co_{0.2}O_2$ powders were synthesized using different chelating agents through sol–gel technique. The impact of

* Corresponding author. Tel.: +98 21 6616 5238; fax: +98 21 66005717.
E-mail address: sasgari@sharif.edu (S. Asgari).

0378-7753/$ – see front matter © 2010 Elsevier B.V. All rights reserved.
doi:10.1016/j.jpowsour.2010.06.097

Table 1
List of materials used in this work.

Material	Company
$LiNO_3$	Riedel-De Haën
$Ni(NO_3)_2{\cdot}6H_2O$	MERCK
$Co(NO_3)_2{\cdot}6H_2O$	MERCK
Triethanolamine (TEA)	ACROS
Citric acid	MERCK
Oxalic acid	MERCK

process parameters such as time and temperature on crystal structure of the powders were studied and electrochemical properties of selected powders were investigated.

2. Experimental

The synthesis of $LiNi_{0.8}Co_{0.2}O_2$ powders was carried out by sol–gel method using materials listed in Table 1. The stoichiometric values of lithium, nickel and cobalt nitrate salts in a cationic ratio of Li:Ni:Co equal to 1:0.8:0.2 were dissolved in distilled water. Three chelating agents including triethanolamine (TEA), citric acid, oxalic acid are used in this investigation. These agents were used in a molar ratio of 1 with respect to the total metal cations by dissolving in distilled water. The solution was then added to the nitrate solution and was heated under constant stirring at 80 °C for 1 h. The resulting sol was heated at 100 °C to form the gel which was dried subsequently. To remove the moisture and achieve the dried mass, the obtained gel was successively dried at 100, 120, 150, 200 °C for 2 h per each step and 5 h at 240 °C. The thermal behavior of $LiNi_{0.8}Co_{0.2}O_2$ powders was determined by thermogravimetric/differential thermal analysis (TG/DTA) conducted on the dried gel at a heating rate of 5 °C min^{-1} up to 1100 °C in the air using a Perkin Elmer analyzer. The tests were conducted in the air using alumina pans. The initial sample weights for TEA, oxalic and citric were 460, 250 and 290 mg, respectively. The dried mass was heated at 500, 600, 700, 800 and 900 °C for varying durations and slowly cooled to room temperature. Inductively coupled plasma (ICP) analysis was performed using an ARL 3410 unit to confirm the stoichiometry of lithium, nickel and cobalt in the synthesized powders. The resulting powders had molar ratios of Li:Ni:Co in the order of 1:0.8:0.2, respectively.

Structural and phase analysis of the resulting powders were carried out by X-ray diffraction (XRD) using a nickel-filtered Cu Kα radiation ($\lambda = 1.5451$ Å) with a scan rate of 2 degree per minute for the whole spectra ($15° \leq 2\theta \leq 80°$) using a Siemens D-500 unit. The morphology, particle size, distribution and structure of $LiNi_{0.8}Co_{0.2}O_2$ powders were examined by a Philips CM 200 TEM/STEM system operating at an accelerating voltage of 200 kV.

Synthesized powders were thoroughly washed and completely dried to remove remaining carbon. This is necessary since high amounts of carbon in the cathode material block the access for lithium ions and deteriorate the electrochemical properties. Batteries were then assembled in argon atmosphere using lithium foil as anode, a microporous polyethylene as separator, 1 M solution of $LiClO_4$ in 50:50 (volume ratio) mixture of ethylene carbonate (EC) and dimethyl carbonate (DMC) as electrolyte and the synthesized compound as cathode material. The cathode was fabricated by blade-coating of a mixture of $LiNi_{0.8}Co_{0.2}O_2$ powders, carbon and PVdF with a weight percent ratio of 90:5:5, respectively. A slurry of this mixture was made using *N*-methy l-2-pyrrolidone (NMP) and was coated on an aluminum foil. After drying overnight at 100 °C, the coated foil was then maintained in a vacuum oven for 2 h at 100 °C. Thin discs 13 mm in diameter were punched out from the dried coating and were used as cathode. The assembled batteries were cycled at constant current densities of 1 (1 C rate) and 0.1 mA cm^{-2} (0.1 C rate) between 3.0 and 4.2 V in a battery cycling tester unit.

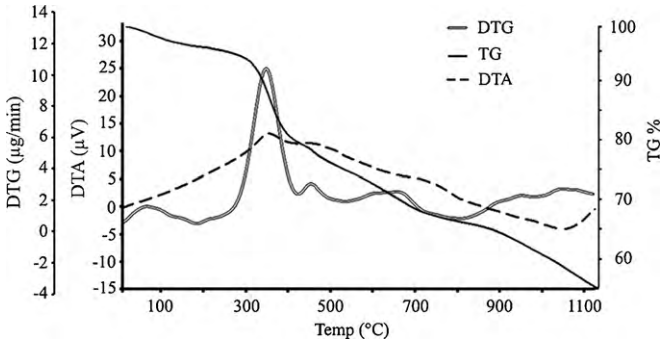

Fig. 1. TG/TGA/DTA data for TEA produced gel precursor.

3. Results and discussion

3.1. Thermal analysis

Fig. 1 shows results of thermogravimetry and differential thermal analysis (TG/DTA) tests taken from dried gel of $LiNi_{0.8}Co_{0.2}O_2$ with TEA as chelating agent. The first weight loss step which persists up to 230 °C is attributed to the removal of residual water molecules in the dried gel. It is however clear that the major portion of weight loss occurs in the range of 100–200 °C. The second step between 230 and 420 °C is related to the burning of organic and nitrate components contained in the precursor. Metal hydroxides in the gel react with organic complexes to produce metal oxides together with the release of NO_x and CO_x gases. The next weight loss around 450 °C is attributed to the initiation of the crystallization reaction. At this temperature, a solid solution with a composition of $Li_xM_{2-x}O_2$ begins to form and redundant components are released in the form of gas [36]. The final step around 680 °C occurs due to the completion of formation of $LiNi_{0.8}Co_{0.2}O_2$ with layered structure. At this temperature, x increases to about 1 in $Li_xM_{2-x}O_2$ and the formation of $LiMO_2$ layered structure is completed by the diffusion of lithium ions. Therefore, M^{2+} in primary MO is oxidized to M^{3+} in the final layered structure. This was confirmed by XRD results that show the best characteristics at about 700 °C where the formation reaction is expected to have been completed.

Differential thermogravimetry (DTG) and DTA data shown in Fig. 1 correspond to the same temperature range and show characteristic peaks close to the temperatures where weight loss occurred. In DTA curve, there is an exothermic peak at 350 °C related to the burning of the organic and nitrate components. These components include the initially added chelating agents. Chelating agents generally facilitate the formation of metal ligand chains between M(Ni,Co)–O and COO^- in carboxylic acids group resulting in the formation of particles at relatively low temperatures with superior morphological characteristics. This process is required for high electrochemical performance. Also, the chelating agent provides the combustion heat required for the synthesis of powders [37,38]. Therefore, if the chelating agent quantity is too small, more segregation of cations occurs and the combustion heat becomes insufficient for the synthesis of powders. On the other hand, excessive amounts of chelating agent may raise the temperature too high in a short period of time and decrease the partial pressure of oxygen near the powders due to the formation of CO and CO_2. Too much formation of CO will reduce the M ions and favor the formation of undesired metal oxides [39]. Chelating agents may also influence the activation energy of formation reactions. The higher the activation energy, the higher the synthesis temperature [40]. In this research,

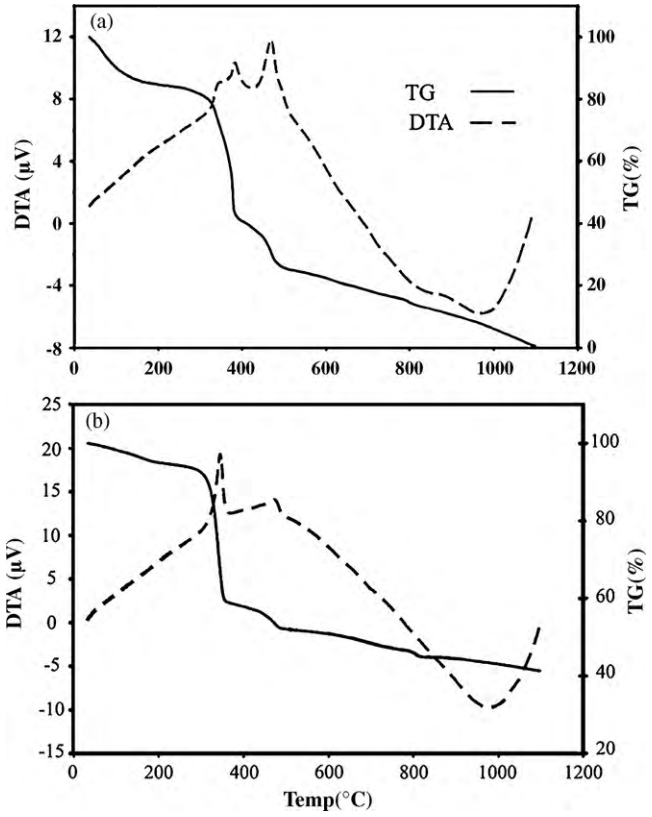

Fig. 2. TG/DTA data for (a) oxalic acid – $LiNi_{0.8}Co_{0.2}O_2$ gel precursor, (b) citric – $LiNi_{0.8}Co_{0.2}O_2$ gel precursor [41,42].

the stoichiometric amounts of all chelating agents were chosen to be in the molar ratio of 1 with respect to all cations present.

As seen in Fig. 1, following the large peak due to burning of nitrate components, two small peaks appear in DTG curve at about 450 and 700 °C. The first peak is attributed to the initiation of the decomposition reaction to form $LiNi_{0.8}Co_{0.2}O_2$, and the second peak is related to the completion of the ordering of the hexagonal lattice. This is in contrast to the data reported previously for oxalic and citric acids as chelating agents which proposed 800 °C as the temperature required for completion of ordering [41,42], as shown in Fig. 2. This is in agreement with the proposal by Delmas et al., who suggested that synthesis of $LiNiO_2$ systems at temperatures higher than 700 °C produced 2D-type cationic ordering structure [18].

In the sample processed by TEA, the total weight loss at 700 °C was about 34%. Also, from Fig. 2a and b the total weight loss at 800 °C are about 82 and 57%, respectively. This significant difference may be attributed to the residual carbon contents in these samples. It is reported that higher amounts of residual carbon prevent agglomeration and particles growth leading to a smaller size distribution of the final particles [43].

3.2. XRD studies

Figs. 3–5 show the results of XRD tests obtained in this study. Fig. 3a–e shows XRD patterns of TEA processed powder (TPP) at different temperatures. Note that those peaks attributed to NiO, CoO, and Li_2CO_3 at 500 °C disappear at higher temperatures. This is concurrent with the increase in the intensity of $LiNi_{0.8}Co_{0.2}O_2$ peaks. It may be concluded that $LiNi_{0.8}Co_{0.2}O_2$ gradually grows at the expense of NiO, CoO, and Li_2CO_3 [44]. On the other hand, with the increase in temperature from 500 to 700 °C, broad peaks become sharper implying an improvement in the crystallinity of the mate-

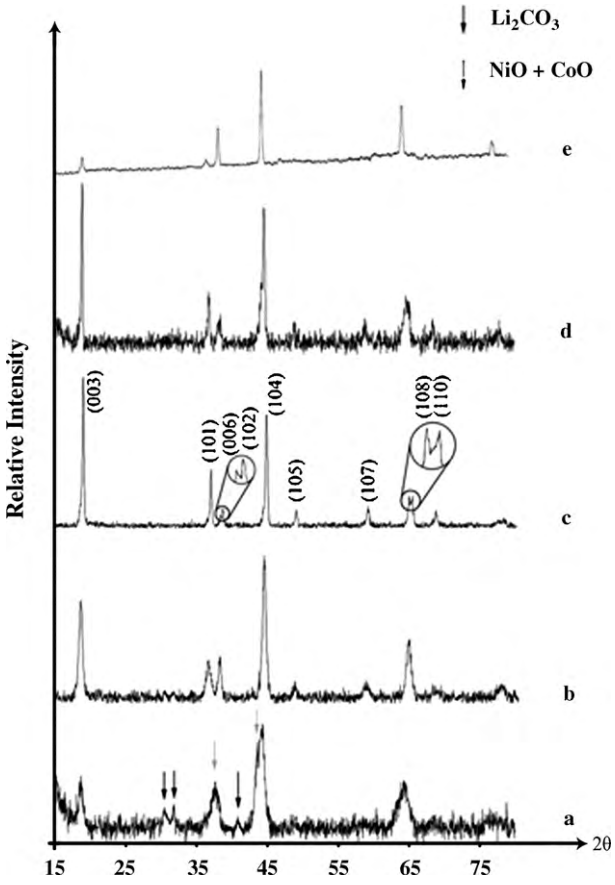

Fig. 3. XRD patterns for TEA processed powders for 8 h at (a) 500 °C, (b) 600 °C, (c) 700 °C, (d) 800 °C and (e) 900 °C.

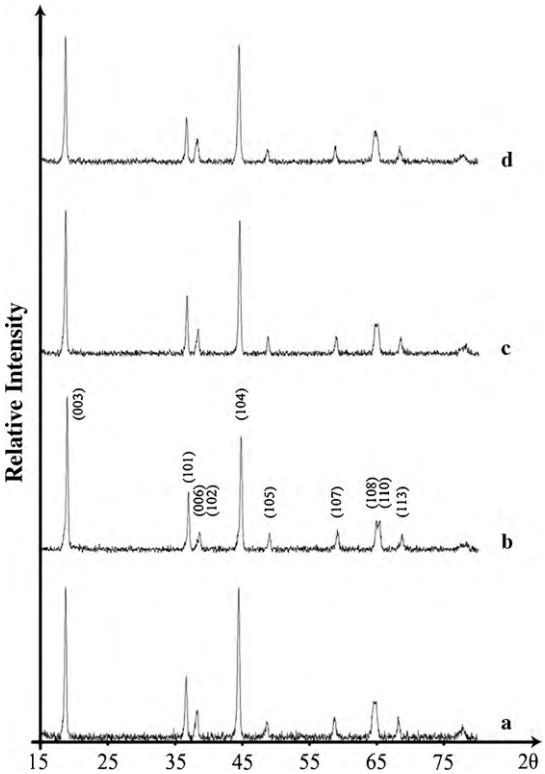

Fig. 4. XRD patterns for TEA processed powders at 700 °C (a) 4 h, (b) 8 h, (c) 12 h and (d) 16 h.

Table 2
Unit cell characteristics and extracted data from XRD patterns for TEA processed powders calcinated for 8 h at different temperatures.

Temp. for 8 h	a (Å)	c (Å)	c/a	V (Å^3)	R	$I_{(003)}/I_{(104)}$
600 °C	2.876	14.241	4.951	102.011	0.95	0.70
700 °C	2.855	14.043	4.918	99.12	0.48	1.33
800 °C	2.868	14.136	4.929	100.696	0.94	0.95

Table 3
Unit cell characteristics and extracted data from XRD patterns for TEA processed powders calcinated at 700 °C for different time.

Time at 700 °C	a (Å)	c (Å)	c/a	V (Å^3)	R	$I_{(003)}/I_{(104)}$
4 h	2.866	14.214	4.959	101.11	0.63	0.91
8 h	2.855	14.043	4.918	99.12	0.48	1.33
12 h	2.865	14.154	4.940	100.61	0.57	1.08
16 h	2.865	14.199	4.956	100.93	0.74	0.98

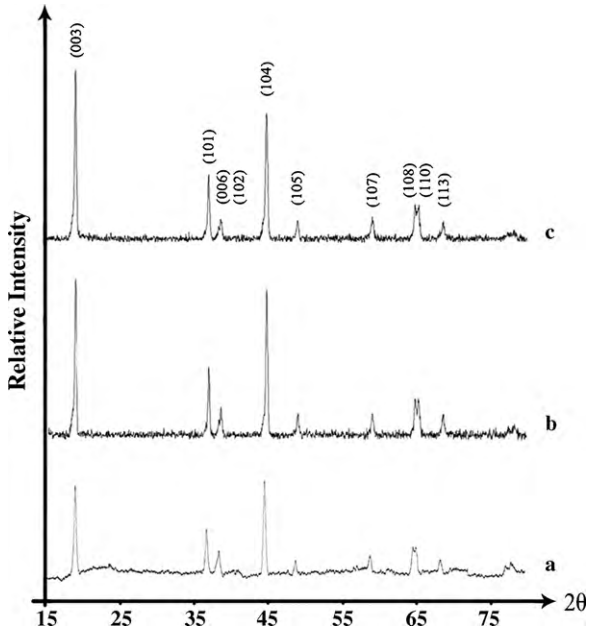

Fig. 5. XRD patterns of $LiNi_{0.8}Co_{0.2}O_2$ prepared using (a) citric acid at 800 °C for 8 h, (b) oxalic acid at 800 °C for 8 h and (c) TEA at 700 °C for 8 h.

rial. Fig. 3c shows the best XRD result obtained in this work from TPP at 700 °C for 8 h. This sample is a single phase $LiNi_{0.8}Co_{0.2}O_2$ of α-$NaFeO_2$ type with space group $R\bar{3}m$. The unit cell is rhombohedral showing trigonal symmetry similar to that proposed by Li et al. [12]. Fig. 4a–d shows XRD results obtained from powders synthesized at 700 °C for different times. Tables 2 and 3 show the data extracted from Figs. 3a–e and 4a–d, respectively. In this table, a and c are the hexagonal lattice parameters and V shows the volume of the unit cell. The R-factor indicates the $(I_{(006)} + I_{(102)})/I_{(101)}$ ratio, as defined by Reimers et al. [45]. This factor decreases with the improvement of hexagonal ordering. It is also known that electrochemical properties are improved as the $I_{(003)}/I_{(104)}$ ratio is increased [46]. According to Table 2, for different temperatures used in this study, the best intensity ratios in TPP samples occur at 700 °C, as confirmed by TG/DTA data (Fig. 1). Also, as seen in Table 3, for different calcination times at 700 °C used in this study, 8 h yields the best result. This may be justified as follows. The diffusion of lithium ion to the oxide lattice increases the x value of the compound $Li_xM_{2-x}O_2$. The corresponding changes in the oxidation state causes the average cationic radius to become smaller ($r_{Li}{}^{+} + r_M{}^{3+} < r_M{}^{2+}$) leading to a decrease in d-spacing and the corresponding increase in the Bragg angle [47]. On the other hand, with increasing calcination time, the intensity ratio of $I_{(003)}/I_{(104)}$ decreases and R increases. This may be attributed to the disturbance of the layered structure and the decrease of hexagonal ordering, in agreement with the increase in the unit cell volume. Also, desirable cation ordering is manifested by the well-separated (1 0 8)–(1 1 0) and (0 0 6)–(1 0 2) peaks [48], as seen in Figs. 3c and 4b.

Fig. 5a–c shows the XRD patterns obtained from samples synthesized with different chelating agents. Fig. 5a–c shows RD results for citric acid, oxalic acid and TPP, respectively. Powder synthesized with oxalic acid and citric acid were calcinated at 800 °C as demonstrated in Section 3.1. Table 4 summarizes the extracted data from Fig. 5a–c. It is seen that TPP has the lowest R value, the highest $I_{(003)}/I_{(104)}$ ratio and the smallest unit cell volume, indicative of desirable hexagonal ordering and electrochemical properties.

3.3. TEM studies

Fig. 6a exhibits TEM image of TPP with an average size of about 50 nm and a fairly narrow size distribution. Fig. 6b and c, on the other hand, shows particles synthesized using oxalic and citric acid, respectively, with an average size of about 1 μm. Fig. 6d presents diffraction pattern of a single particle of $LiNi_{0.8}Co_{0.2}O_2$ which shows hexagonal lattice in agreement with XRD data.

The remarkable difference between the sizes of particles in Fig. 6a compared to those in Fig. 6b and c may be explained as follows. TEA ($N(C_2H_4OH)_3$) is an alkanolamine with a high tendency to produce stable transition metal complexes [49,50]. This prevents rapid hydrolysis and condensation in presence of water leading to homogeneous gel formation and therefore smaller particle size. Furthermore, TEA is also used as a surfactant in many reactions to prepare well dispersed powders [51]. On the other hand, TEA helps metal ions remain in the solution and provides sufficient flexibility to the system to exist homogeneously throughout the evaporation process without undergoing any precipitation and segregation. The evolution of various gases accompanying the decomposition stage makes the structure highly porous and fluffy. This facilitates disin-

Table 4
Unit cell characteristics and extracted data from XRD patterns for $LiNi_{0.8}Co_{0.2}O_2$ powders synthesized using different chelating agents.

Chelating agent	a (Å)	c (Å)	c/a	V (Å^3)	R	$I_{(003)}/I_{(104)}$
Citric	2.868	14.128	4.926	100.64	0.76	0.96
Oxalic	2.859	14.079	4.924	99.66	0.72	0.97
TEA	2.855	14.043	4.918	99.12	0.48	1.33

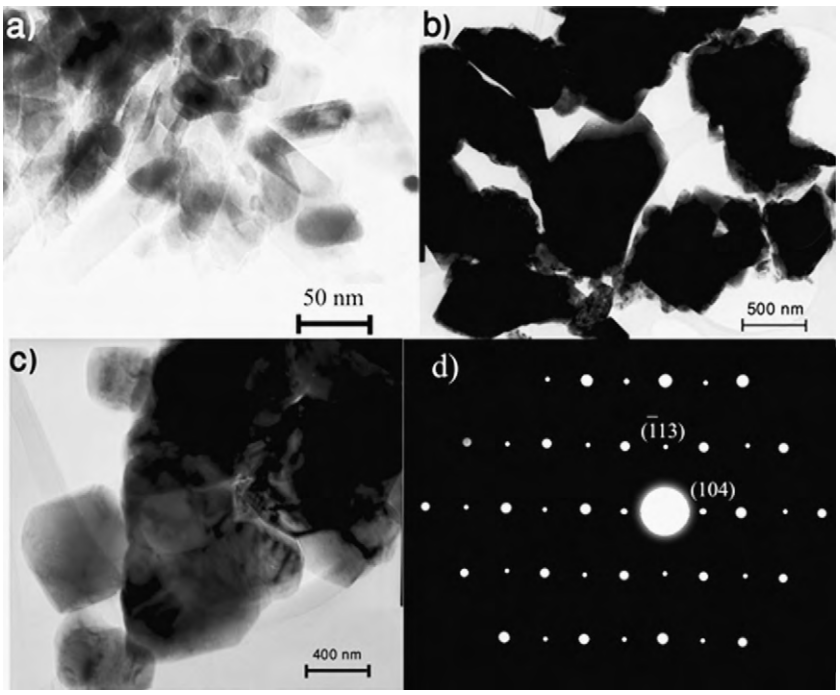

Fig. 6. TEM images of $LiNi_{0.8}Co_{0.2}O_2$ particles produced by (a) TEA, (b) citric acid and (c) oxalic acid. (d) Diffraction pattern of a single crystal of $LiNi_{0.8}Co_{0.2}O_2$.

tegration of the agglomerated particles and inhibits further growth of these particles [52]. The amount of residual carbon may also influence the resulting particle size, as mentioned in Section 3.1.

We have also studied the influence of calcination temperature on growth of TPP in the range of 700–800 °C (for 8 h). TEM results showed a small increase in average particle size from 50 nm to about 58 nm in this range. XRD results (Table 2), however, showed a degradation of the crystal structure with increasing temperature from 700 to 800 °C. Based on these results, the optimized calcination temperature for TPP was selected as 700 °C.

3.4. Electrochemical properties

Batteries were assembled using $LiNi_{0.8}Co_{0.2}O_2$ powders synthesized with different chelating agents and were then tested. Figs. 7 and 8 show the results of discharge capacity vs. cycle number with discharge currents of 0.1 and 1 C rate, respectively. According to Fig. 7, the discharge capacity of the first cycle for TPP is 173 mAh g^{-1} and for the twentieth cycle is 166. Therefore, it shows a capacity retention equal to 95%. For Citric and Oxalic capacity retention after twenty cycles are approximately 92 and 91%. In Fig. 8, the first and twentieth discharge cycle capacities of TPP are equal to 157 and 134 mAh g^{-1}, respectively, implying a capacity retention of 85%. Also, Oxalic and Citric showed capacity retention of 65 and 59%, respectively. In both Figs. 7 and 8, TPP shows higher capacity and better electrochemical properties than those synthesized by Oxalic and Citric acid. This is in agreement with XRD results discussed earlier (Section 3.2). It should be noticed that batteries cycled at the 0.1 C have higher first discharge capacities and superior capacity retentions compared to those cycled at 1 C. It is clear that for all cathode powders, capacity loss is larger at higher charge–discharge rate (1 C). This may be related to the internal resistance of the cell due to the formation of passive films and cathode–electrolyte reactions. These processes are accelerated with increasing discharge rate. Also, increasing the discharge rate may raise the temperature and degrade the performance of the cell [53,54]. The capacity loss for TPP is, however, lower than that of others. This is attributed to the crystal structure as discussed in Section 3.2 on XRD data. Also, data presented in Figs. 7 and 8 imply

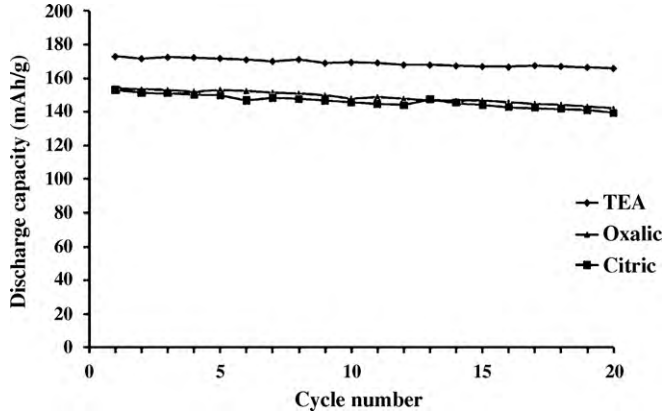

Fig. 7. Discharge curves for $LiNi_{0.8}Co_{0.2}O_2$ prepared by different chelating agents with constant current density of 0.1 C rate, within the voltage range of 3–4.2 V.

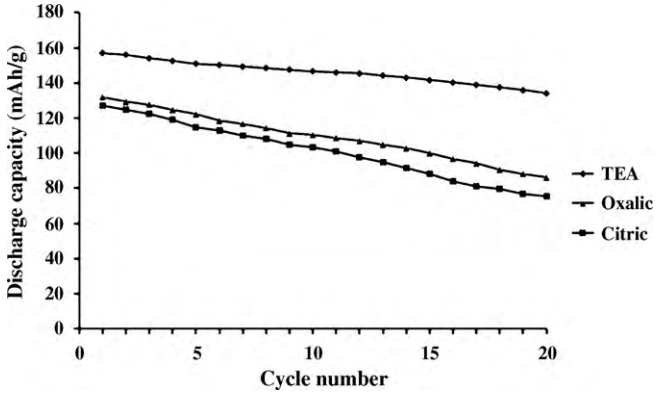

Fig. 8. Discharge curves for $LiNi_{0.8}Co_{0.2}O_2$ prepared by different chelating agents with constant current density of 1 C rate, within the voltage range of 3–4.2 V.

a better rate capability for nano-sized particles of TPP. This has been related to the larger surface area and reduced path length of nano-sized particles [33,34,55]. The enhancement of rate capability is a desirable achievement in Li-ion battery industry since fast lithium ion transport cycle reduces the charging time of these batteries in portable devices. Data presented in this work may be used to improve the electrochemical properties of Li-ion batteries.

4. Conclusions

1. Of TEA, citric and oxalic acids used as chelating agents, powders produced by TEA showed better properties. While powders synthesized by citric and oxalic acids were in the micron size range, TEA produced nanopowders with a narrow size distribution.
2. The optimal heat treatment for synthesis of powders by TEA was obtained at 700 °C for 8 h as confirmed by TG/DTA and XRD results.
3. Assembled batteries using powders produced by TEA showed superior electrochemical properties such as higher discharge capacity, better rate capability and improved capacity retention compared to that of particles produced by oxalic and citric agents. These characteristics are attributed to better hexagonal ordering and nano-sized particles of the powders used as cathode material.

Acknowledgements

Authors would like to thank Sharif University of Technology for financial support of this work. Also, Ms. P. Amini is gratefully acknowledged for preparing TEM samples.

References

[1] K. Mizushima, P.C. Jones, P.J. Wiseman, J.B. Goodenough, Mater. Res. Bull. 15 (1980) 783.
[2] T. Nagaura, K. Tazawa, Prog. Batteries Solar Cells 9 (1990) 209.
[3] T. Ohzuku, A. Ueda, J. Electrochem. Soc. 141 (1994) 2972.
[4] J.R. Dahn, U. von Sacken, M.R. Jukow, H. Al-Janaby, J. Electrochem. Soc. 138 (1991) 2207.
[5] T. Ohzuku, A. Ueda, M. Nagayama, J. Electrochem. Soc. 140 (1993) 1862.
[6] J.R. Dahn, U. von Sacken, C.A. Michel, Solid State Ionics 44 (1990) 87.
[7] T. Nohma, H. Kurokawa, M. Uehara, M. Takahashi, K. Nishio, T. Saito, J. Power Sources 54 (1995) 522.
[8] R.J. Gummow, A. de Kock, M.M. Thackeray, Solid State Ionics 69 (1994) 59.
[9] G. Amatucci, A. Du pasquier, A. Blyr, T. Zheng, J.-M. Tarascon, Electrochim. Acta 45 (1999) 255.
[10] A. Rougier, I. Saadoune, P. Gravereau, P. Willmann, C. Delmas, Solid State Ionics 90 (1996) 83.
[11] B.J. Neudecker, R.A. Zuhr, B.S. Kwak, J.B. Bates, J. Electrochem. Soc. 145 (1998) 4161.
[12] W. Li, J.N. Reimers, J.R. Dahn, Solid State Ionics 67 (1993) 123.
[13] C. Delmas, I. Saadouns, Solid State Ionics 53–56 (1992) 370.
[14] Z. Lu, J.R. Dahn, J. Electrochem. Soc. 149 (2002), A 815.
[15] J.-S. Kim, C.S. Johnson, M.M. Thackeray, Electrochem. Commun. 4 (2002) 205.
[16] I. Saadoune, C. Delmas, J. Mater. Chem. 6 (1996) 193.
[17] W. Li, J. Curie, J. Electrochem. Soc. 144 (1997) 1773.
[18] C. Delmas, M. Menetrier, L. Croguennec, I. Saadoune, A. Rougier, C. Pouillerie, G. Prado, M. Grune, L. Fournes, Electrochim. Acta 45 (1999) 243.
[19] J. Cho, H. Jung, Y. Park, G. Kim, H.S. Lim, J. Electrochem. Soc. 147 (2000) 15.
[20] C. Delmas, I. Saadoune, A. Rougier, J. Power Sources 43–44 (1993) 595.
[21] J. Aragane, K. Matsui, H. Andoh, S. Suzuki, F. Fukuda, H. Ikeya, K. Kitaba, R. Ishikawa, J. Power Sources 68 (1997) 13.
[22] J.M. Tarascon, M. Armand, Nature 414 (2001) 361.
[23] M. Winter, J.O. Besenhard, M.E. Spahr, P. Novak, Adv. Mater. 10 (1998) 743.
[24] R. Alcantara, P. Lavela, J.L. Tirado, E. Zhecheva, R. Stoyanova, J. Solid State Electrochem. 3 (1999) 126.
[25] K.K. Lee, K.B. Kim, J. Electrochem. Soc. 147 (2000) 1709.
[26] J. Cho, Chem. Mater. 12 (2000) 3089.
[27] S. Venkatraman, Y. Shin, A. Manthiram, Electrochem. Solid State Lett. 6 (2003) 9.
[28] T. Tsumura, A. Shimizu, M. Inagaki, J. Mater. Chem. 3 (1993) 1995.
[29] Y. Gao, J.R. Dalin, J. Electrochem. Soc. 143 (1996) 100.
[30] P. Barboux, J.M. Tarascon, F.K. Shokoohi, J. Solid State Chem. 94 (1991) 185.
[31] W. Liu, G.C. Farrington, F. Chaput, B. Dunn, J. Electrochem. Soc. 143 (1996) 879.
[32] B.J. Hwang, R. Santhanam, D.G. Liu, J. Power Sources 101 (2001) 86.
[33] N. Li, C.R. Martin, B. Scrosati, J. Power Sources 97–98 (2001) 240.
[34] T. Kawamura, M. Makidera, S. Okada, K. Koga, N. Miura, J. Yamaki, J. Power Sources 146 (2005) 27.
[35] D. Larcher, C. Masquelier, D. Bonnin, Y. Chabre, V. Masson, J.B. Leriche, J.M. Tarascon, J. Electrochem. Soc. 150 (1) (2003) 133.
[36] P. Kalyani, N. Kalaiselvi, Sci. Technol. Adv. Mater. 6 (2005) 689.
[37] Y.s. Lee, Y.K. Sun, K.S. Nahm, Solid State Ionics 109 (1998) 285.
[38] Y.K. Sun, Solid State Ionics 100 (1997) 115.
[39] S. choi, A. Manthiram, J. Electrochem. Soc. 147 (2000) 1623.
[40] G. Ting-Kuo Fey, Jian-Ging Chen, Zhi-Feng Wang, Hao-Zhong Yang, T. Prem Kumar, Mater. Chem. Phys. 87 (2004) 246.
[41] S. Soltan Mohamad, Effects of sol–gel parameters on the size and morphology of nanopowders of Li–Co oxide, Sharif University of Technology, M.Sc. Thesis, Deparment of Materials Science and Engineering, 2009.
[42] M. Balande, Effects of sol–gel parameters on the size and morphology of nanopowders of Li–Ni oxide, Sharif University of Technology, M.Sc. Thesis, Deparment of Materials Science and Engineering, 2008.
[43] V. Subramanian, Kishor Karki, B. Rambabu, Solid State Ionics 175 (2004) 315.
[44] Y.D. Zhong, X.B. Zhao, G.S. Cao, J.P. Tu, T.J. Zhu, J. Alloys Compd. 420 (2006) 298.
[45] J.N. Reimers, E. Rossen, C.D. Jones, J.R. Dahn, Solid State Ionics 61 (1993) 335.
[46] T. Ohzuku, A. Ueda, M. Nagayam, I. Iwakishi, H. Komori, Electrochim. Acta 38 (1993) 1159.
[47] A. Hirano, R. Kanno, Y. Kawamoto, Y. Takeda, K. Yamaura, M. Takano, K. Ohyama, M. Ohashi, Y. Yamaguchi, Solid State Ionics 78 (1995) 123.
[48] G. Ting-Kuo Fey, Jian-Ging Chen, Zhi-Feng Wang, Hao-Zhong Yang, T. Prem Kumar, Mater. Chem. Phys. 87 (2004) 246.
[49] Asit Baran Panda, Amita Pathak, Makhanlal Nandagoswami, Mater. Sci. Eng. B 97 (2003) 275.
[50] Tanja Kocareva, Ivan Grozdanov, Biljana Pejova, Mater. Lett. 47 (2001) 319.
[51] S.B. Rane, T. Seth, G.J. Phatak, Mater. Lett. 57 (2003) 3096.
[52] Asit B. Panda, Amita Pathak, Panchanan Pramanik, Mate. Lett. 52 (2002) 180.
[53] Gang Ning, Bala Haran, Branko N. Popov, J. Power Sources 117 (2003) 160.
[54] J. Li, E. Murphy, J. Winnick, P.A. Kohl, J. Power Sources 102 (2001) 294.
[55] L.F. Nazar, G. Goward, F. Leroux, M. Duncan, H. Huang, T. Kerr, J. Gaubicher, Int. J. Inorg. Mater. 3 (2001) 191.